

# Electromagnetic Vibrational Energy Harvesting Using Boost And Buck Boost Converter

G. Sridhar Babu<sub>M.Tech</sub>  
Assistant Professor,  
Department of EEE,  
St. Martin's Engineering  
College, Hyderabad.

Vishal Mishra  
Department of EEE,  
St. Martin's Engineering  
College, Hyderabad.

G. Suresh Kumar  
Department of EEE,  
St. Martin's Engineering  
College, Hyderabad.

**Abstract** - In this project, electromagnetic generators are used to harvest the energy present in ambient vibrations. The harvesting is done using Boost and Buck-Boost converters. These are used for direct AC-DC conversion without using the front-end bridge rectifier as the bridge rectification is inefficient and is not practical for low voltage micro generators. The proposed converter consists of the above two converters which are connected in parallel and are operated in the positive and negative half cycles respectively. They are operated in the discontinuous mode to minimize the losses as they are significant in the conversion of low voltage ac to the required dc voltage. Analysis of the converters is carried out to obtain the relation between the power and the duty cycle of the converter. A self starting circuit is proposed for independent operation of the converter. Simulation results are presented to validate the proposed converter.

## 1. INTRODUCTION

The recent development of compact and low powered electronic devices has enabled the development of self-powered devices. The traditional use of batteries for such devices is undesirable due to limited shelf life and replacement accessibility. To avoid this, inertial microgenerators are used which harvest vibrations from the ambience and convert into electrical energy. The voltage obtained is very low and it cannot be used in practical applications. To make it practically usable, the voltage is boosted to higher values using power

electronic devices such as boost and buck-boost converters. Also, the conversion from ac-dc is done with the same circuit which meets our requirement to operate low power electronic devices.

## 2. INERTIAL MICRO-GENERATORS

Among the different types of inertial micro-generators, electromagnetic micro-generators are used in this paper.

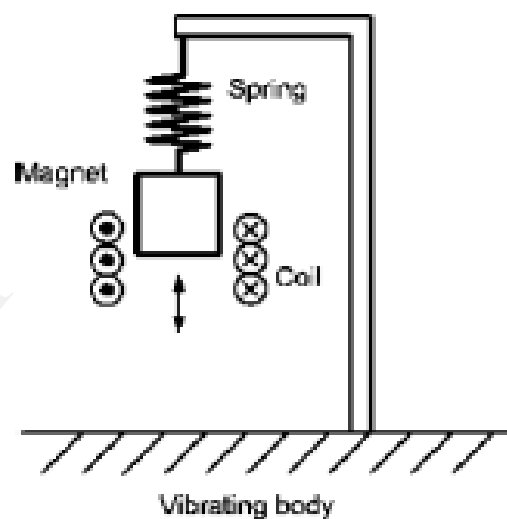


Fig.1. Electromagnetic Micro-generator

The electromagnetic microgenerators work on the principle of Faraday's laws of electromagnetic induction. It consists of a stationary coil and a permanent magnet. The magnet is kept free in air with the help of spring so that it allows free movement due to which it is able to move due to the ambient vibrations. Due to this rotation, emf is induced in the coil. The output voltage of these microgenerators is only few millivolts and it is alternating in nature. Most of the electronic devices typically require a dc voltage of 3.3V. so the emf induced is rectified and stepped up to the required voltage with the help of power converters.

## 3. CONVENTIONAL POWER CONVERTER

The conventional power converter consists of two stages: a diode bridge rectifier and a standard Buck or Boost converter dc-dc converter. However the bridge rectification is not feasible for low voltage micro-generators

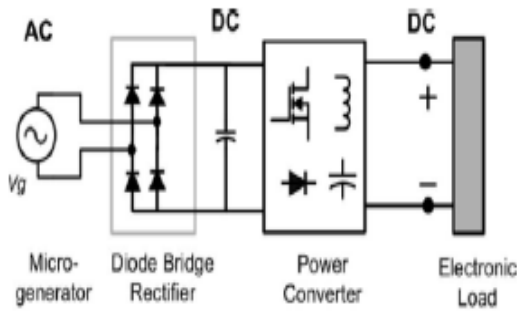


Fig.2-Conventional Power Converter

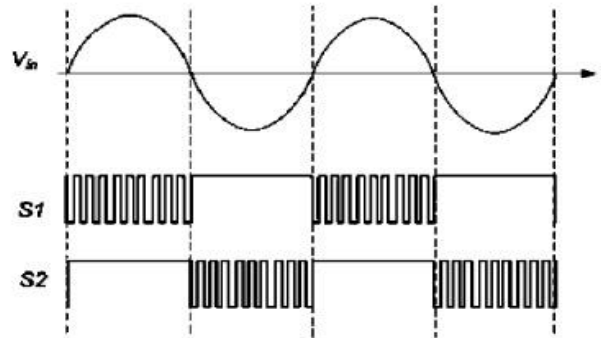


Fig.4 (b) Input Voltage and Gate Drive Pulses

and if feasible, the power conversion is very inefficient due to the forward voltage drops in diodes. In order to avoid the problems of two-stage power conversion, direct ac-to-dc power converters are proposed, in which the ac output voltage of microgenerators is processed by a single stage boost type converters.

**4. Single Stage AC-DC Converter**

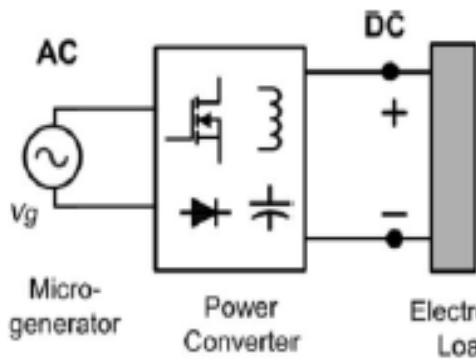


Fig. 3-Single Stage AC-DC Power Converter

The proposed converter consists of a boost converter in parallel with buck-boost converter which are operated in the positive and negative half cycles respectively. The output dc bus is realized by using a single capacitor. The standard 2-switch H-bridge converter is as shown in the fig.4(a) which can be used for the direct ac-dc boost conversion. The waveform of input voltage and the gate drive pulses of the lower switches are as shown in fig 4(b). It can be seen that during positive half cycle switch S2 is kept ON for the entire half cycle and the gate

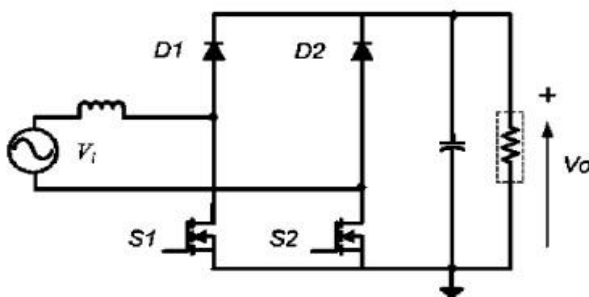


Fig.4 (a) H-Bridge Configuration

pulse to S1 is controlled and during the negative half cycle, the switch S1 is kept ON for the entire half cycle and the gate pulse to S2 is controller. However, there are various disadvantages in these H-bridge converters. Firstly, during charge and discharge of inductors there are always two devices in the conduction path whereas in the proposed converter there is only one switch in the conduction path during the entire half cycle. So, the device conduction losses are reduced by a factor of two in the proposed converter. Second, in the H-bridge topologies, the implementation of control scheme is difficult due to the floating of input voltage source with respect to ground. Third, as the MOSFET switches are designed for forward conduction, they offer higher on-state resistance in the reverse conduction mode. So, due to these problems associated with the H-bridge configuration, it is not preferred.

**5. WORKING OF ENERGY HARVESTING CIRCUIT**

The electromagnetic microgenerators typically consist of a moving permanent magnet, linking flux with a stationary coil (see Fig. 1). The variation of the flux linkage induces ac voltage in the coil. In this paper, microgenerator output voltage is modelled as a sinusoidal voltage source.

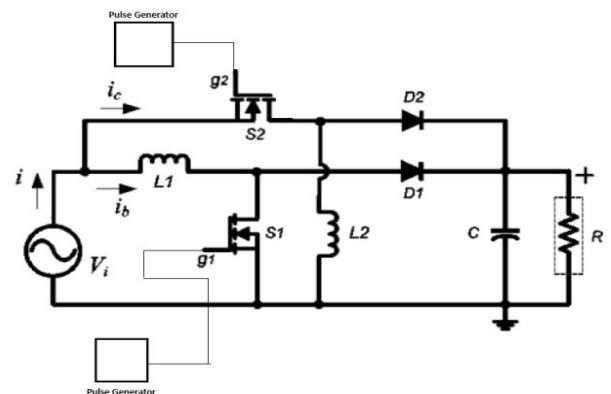


Fig.5 Proposed Direct AC-DC Converter

The proposed direct ac-to-dc circuit is as shown in the fig.5. It consists of boost converter in parallel with the buck boost converter. The output capacitor C is charged by the boost converter (comprising of inductor L1, Switch S1, diode D1) during the positive half cycle and by the buck-boost converter (comprising of inductor L2, Switch S2, diode D2) in the negative half cycle respectively. To block the reverse

conduction, the forward voltage drop of the body diodes of the MOSFETs is chosen to be higher than the peak of the input ac voltage. Two schottky diodes ( $D1$  and  $D2$ ) with low forward voltage drop are used in the boost and the buck–boost converter circuits for low losses in the diodes. The proposed converter is operated under discontinuous mode of operation (DCM). This reduces the switch turn ON and turn OFF losses. The DCM operation also reduces the diode reverse recovery losses of the boost and buck–boost converter diodes. Furthermore, the DCM operation enables easy implementation of the control scheme. It can be noted that under constant duty cycle DCM operation, the input current is proportional to the input voltage at every switching cycle; therefore, the overall input current will be in-phase with microgenerator output voltage. The converter operation can be divided mainly into four modes. Mode-1 and Mode-2 are for the boost converter operation during the positive half cycle of the input voltage. Under Mode-1, the boost switch  $S1$  is ON and the current in the boost inductor builds. During Mode-2, the switch is turned OFF and the output capacitor is charged. The other two modes: Mode-3 and Mode-4 are for the buck–boost converter operation during the negative half cycle of the input voltage. Under Mode-3, the buck–boost switch  $S2$  is ON and current in the buck–boost inductor builds. During Mode-4, the buck–boost switch  $S2$  is turned OFF and the stored energy of the buck–boost inductor is discharged to the output capacitor. The pulses to the gate of the mosfets are given with the help of pulse generators.

6. CONVERTER ANALYSIS

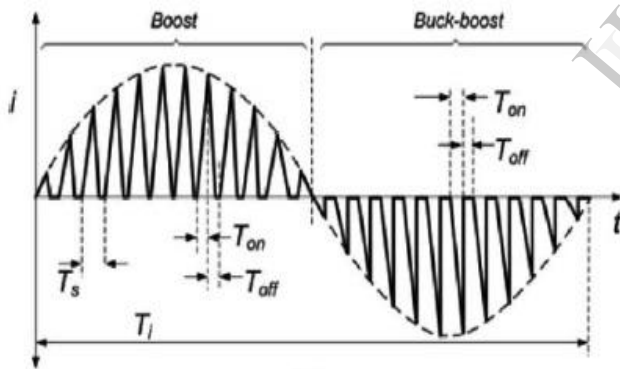


Fig.6 (a) Input Current Waveform of the Converter

Consider the input current waveform of the converter as shown in Fig. 6(a). It can be noted that during the boost converter operation, the input current  $i$  and the boost inductor current ( $iL1$ ) are equal, but during the buck–boost converter operation, the input current  $i$  and the current in buck–boost inductor ( $iL2$ ) are not equal. This is because; in the buck–boost converter, the input current becomes zero.

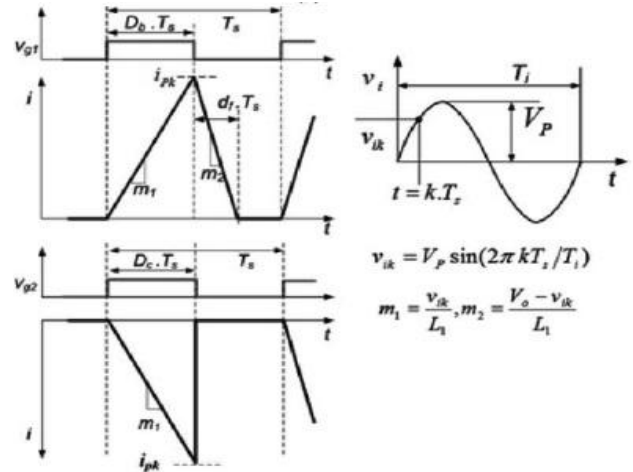


Fig.6 (b) Input currents, gate drive signals and input voltage during a switching cycle of boost and buck–boost converter.

During the switch turn OFF period ( $T_{OFF}$ ). Therefore, in a switching cycle, the energy transferred to the output by a buck–boost converter is equal to the energy stored in the inductor, whereas, in the boost converter, the energy transferred to the output is more than the energy stored in the inductor. Hence, for the equal duty cycles, input voltages and inductor values ( $L1 = L2$ ), the total powers delivered by the two converters over an input voltage cycle are not equal. Consider any  $k$ th switching cycle of the boost and the buck–boost converter as shown in Fig. 6(b), where  $T_s$  is the time period of the switching cycle,  $D_b$  is the duty cycle of the boost converter,  $d_f T_s$  is the boost inductor current fall time (or the diode  $D1$  conduction time),  $D_c$  is the duty cycle of the buck–boost converter,  $v_i$  is the input voltage of the generator with amplitude  $V_p$ , and  $V_o$  is the converter output voltage. Assuming the switching time period ( $T_s$ ) of the converter is much smaller than the time period of the input ac cycle ( $T_i$ ), the peak value of the inductor current ( $i_{Pk}$ ) in the boost converter can be obtained as in (1).

$$i_{Pk} = m_1 D_b T_s = v_{ik} D_b T_s / L_1 \tag{1}$$

where  $v_{ik} = V_p \sin\left(\frac{2\pi k T_s}{T_i}\right)$ .

After the boost converter switch is turned OFF, the current in inductor starts to fall (see Fig. 6). The slope ( $m_2$ ) of this current is decided by the voltage across the inductor. In a  $k$ th switching cycle, the voltage across the inductor during the inductor current fall time is:  $V_0 - v_{ik}$ . Therefore, the inductor current fall time can be found as in Equation (2).

$$d_f T_s = \frac{i_{Pk}}{m_2} = \frac{L_1 i_{Pk}}{V_0 - v_{ik}} \tag{2}$$

During this  $k$ th switching cycle, the total energy ( $E_{kb}$ ) transferred from the input of the boost converter can be obtained as in (3)

$$E_{kb} = \frac{v_{ik} i_{Pk} (D_b + d_f) T_s}{2} \quad (3)$$

The average power supplied in the boost switching cycle is

$$P_{kb} = \frac{E_k}{T_s} = \frac{v_{ik} i_{Pk} (D_b + d_f)}{2} \quad (4)$$

The number of switching cycles during the time period of one input ac cycle is defined as  $N = T_i/T_s$ . In the proposed power electronics converter topology, the boost converter is operated for the half time period of the input ac cycle ( $T_i/2$ ). The average input power  $P_{ib}$  of the boost converter over this half cycle time period can be obtained as in (5)

$$P_{ib} = \left(\frac{2}{N}\right) \sum_{k=1}^{\frac{N}{2}} P_{kb} \\ = \left(\frac{2}{N}\right) \sum_{k=1}^{\frac{N}{2}} \frac{v_{ik} i_{Pk} (D_b + d_f)}{2} \quad (5)$$

For large  $N$ , the discrete function in (5) can be treated as a continuous function. The average input power of the boost converter  $P_{ib}$  (5) can be obtained by integrating the term in the summation over the half cycle ( $T_i/2$ ) period of the input ac voltage and then taking its mean value. The average power of the boost converter expressed in the integration form can be obtained as in (6)

$$P_{ib} \\ = \frac{2}{T_i} \int_0^{T_i/2} \frac{D_b^2 T_s}{2L_1} V_p^2 \sin^2\left(\frac{2\pi}{T_i} t\right) \\ \times V_0 \left( V_0 V_p \sin\left(\frac{2\pi}{T_i} t\right) \right)^{-1} dt \quad (6)$$

Simplifying (6), the average input power for the boost converter  $P_{ib}$  is found to be as follows:

$$P_{ib} = \frac{V_p^2 D_b^2 T_s}{4L_1} \beta$$

$$\text{Where } \beta = \left(\frac{2}{\pi}\right) \int_0^{\pi} \frac{1}{1 - (V_p/V_0) \sin\theta} d\theta$$

$$\text{and } \theta = \frac{2\pi t}{T_i} \quad (7)$$

It can be noted that in (7),  $\beta$  is constant for fixed values of  $V_p$  and  $V_0$ .

In steady state, the average input power of the converter is equal to the sum of the average output power and the various converter losses. Hence, by defining the converter efficiency as

$\eta$  for a load resistance  $R$ , the input power and the output power can be balanced as in (8)

$$\frac{V_p^2 D_b^2 T_s}{4L_1} \beta = \frac{V_0^2}{R} \frac{1}{\eta} \quad (8)$$

From (8), the duty cycle of the boost converter ( $D_b$ ) can be obtained as

$$D_b = \frac{2V_0}{V_p} \sqrt{\frac{L_1}{RT_s \eta} \frac{1}{\beta}} \quad (9)$$

Further, consider the operation of the buck–boost converter; in this case the input power is supplied only during the ON period of the switch  $S_2$  (see Fig. 3). During the OFF period of the switch  $S_2$ , the input current is zero [see Fig. 5(a)]. Hence, for any  $k$ th switching cycle, the average power supplied by the buck–boost converter  $P_{kc}$  can be obtained as

$$P_{kc} = \frac{v_{ik} i_{Pk} D_c}{2} \quad (10)$$

Applying similar approach, used earlier for the boost converter, the average power can be expressed in the integration form as

$$P_{ic} = \frac{2}{T_i} \int_0^{T_i/2} \frac{D_b^2 T_s}{2L_1} V_p^2 \sin^2\left(\frac{2\pi}{T_i} t\right) dt \\ = \frac{V_p^2 D_b^2 T_s}{4L_1} \quad (11)$$

The duty cycle  $D_c$  can be obtained as in (12)

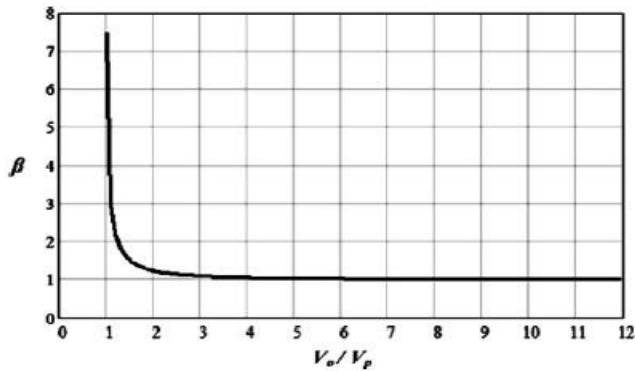
$$D_c = \frac{2V_0}{V_p} \sqrt{\frac{L_2}{RT_s \eta}} \quad (12)$$

## 7. CONTROL SCHEME

Using (9) and (12), the duty cycle of the boost converter  $D_b$  and the duty cycle of the buck–boost converter  $D_c$  can be related as

$$\frac{D_b}{D_c} = \sqrt{\frac{L_1}{L_2} \frac{1}{\beta}} \quad (13)$$

Based on (13), two different control schemes can be proposed for the boost and buck–boost-based converter to deliver equal average input power. In scheme 1, the values of the inductors are kept to be equal ( $L_2 = L_1$ ) and the converters are controlled with different duty cycles such that it satisfies the condition:  $D_c = D_b \sqrt{\beta}$ . In scheme 2, both the boost and the buck–boost converters are controlled with same duty cycle ( $D_b = D_c$ ), whereas the inductor values are chosen to satisfy the condition:  $L_1 = \beta L_2$ . In Fig.6, the variable  $\beta$  from (6) is plotted as a function of the step-up ratio ( $V_0/V_p$ ). It can be seen from this plot that for large values of voltage step-up ratio,  $\beta$  approaches to 1. Hence for higher voltage step-up ratio applications, the boost and the buck–boost converters can be designed

Fig.7- $\beta$  Versus  $V_o/V_p$  (step-up ratio  $>1$ ) Plot.

with inductors of equal values and they can be controlled with the same duty ratio to successfully deliver the required average power to the output. This is assistive for the target application of this study, where the very low voltage is stepped up to a much higher dc output voltage. It can be mentioned that the value of  $\beta$  approaches to infinity for  $V_o/V_p \rightarrow 1$ . Therefore, from (7), the input power for the boost converter may seem to approach infinity as well. But in this case, the duty cycle of the boost converter  $Db$  approaches to zero for  $V_o/V_p \rightarrow 1$ . Therefore, no power is transferred from the input to the output and the equation remains valid even when  $V_o/V_p = 1$ .

## 8. SIMULATION RESULTS

A resonance-based electromagnetic microgenerator, producing 400 mV peak sinusoidal output voltage, with 100-Hz frequency is considered in this study for verification of the proposed converter topology (see Fig. 5). The closed-loop simulation of the converter is carried out based on the control schemes presented in 7. The reference output voltage ( $V_{ref}$ ) is considered to be 3.3 V. The energy-harvesting converter is designed for supplying power to a 200- $\Omega$  load resistance, hence, supplying about 55 mW of output power. The converter design is carried out based on the analysis and design guidelines, discussed earlier in Section 5. Commercially available MOSFET (Si3900DV from Vishay) is selected to realize the switches  $S1$  and  $S2$ . The forward voltage of the selected MOSFET body diode is about 0.8 V, which is higher than the peak of the input voltage. This inhibits any reverse conduction in the MOSFETs. The nominal duty cycle of the converter is chosen to be 0.7. The inductor is designed to have a standard value of 4.7  $\mu$ H and commercially available inductor (IHLP-2525CZ from Vishay) is used to realize  $L1$  and  $L2$ . The diodes,  $D1$  and  $D2$  are chosen to be schottky type with low forward voltage (0.23 V, NSR0320 from ON Semiconductor). The output capacitor value is 68  $\mu$ F. Various values for circuit components of the designed converter are presented in Table I. The buck-boost converter duty cycle  $Dc$  is calculated from the estimated duty cycle  $Db$  and (13). The input current of the boost converter and the input current of the buck-boost converter for load resistance  $R = 200 \Omega$  is shown in Fig. 9(a) and (b), respectively. The total input current and the microgenerator output voltage ( $v_i$ ) are shown in Fig. 10 and Fig.8 respectively. It can be seen that the boost converter is

operated during the positive half cycle, while the buck-boost converter is operated during negative half cycle of the microgenerator output voltage. The converter output voltage and the duty cycles, estimated by the controller are shown in Fig. 12 and Fig.11, respectively. The output voltage ripple is about  $\pm 0.14$ V, which is  $\pm 4.24\%$  of the nominal output voltage. The estimated efficiency of the converter is 63%. For this operating condition, the duty cycle calculated from the analysis of Section 5 is  $Db = 0.71$ . It can be noted from Fig. 11 that the estimated duty cycle by the controller in the circuit simulation closely matches with value of the duty cycle calculated analytically. In this study, the output voltage to input voltage peak step-up ratio is:  $V_o/V_p = 8.25$ . These corroborate the earlier conclusion from the analysis in Section 6 (see Fig. 7) that for high step-up ratio, the duty cycles of the converters with same inductor values will be almost equal. To validate this proposed control scheme, further simulations of the converter is carried out for load resistance  $R = 200 \Omega$  when the boost and buck-boost converter are controlled with same duty ratio. Fig.11, Fig.12 presents the duty cycle and the output voltage of the converter, respectively. To verify the operation of the converter under different load conditions, the load resistance is increased to  $R = 400 \Omega$ . The output voltage under this load condition is shown in Fig.13.

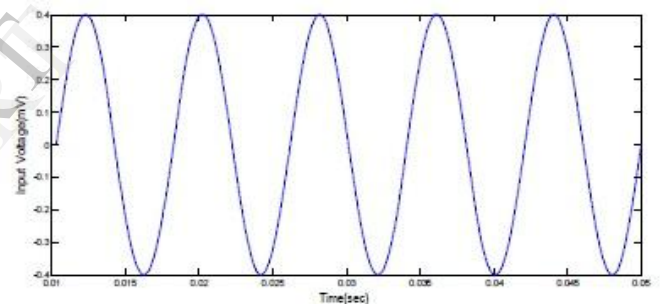


Fig. 8 Input voltage

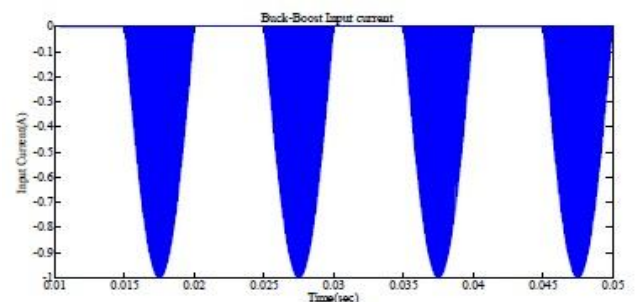
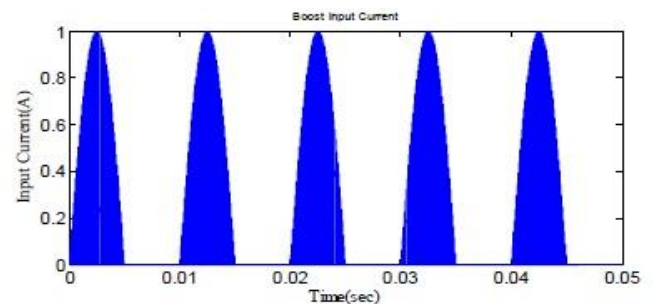


Fig.9 (a) Boost input current (b) buck-boost input current

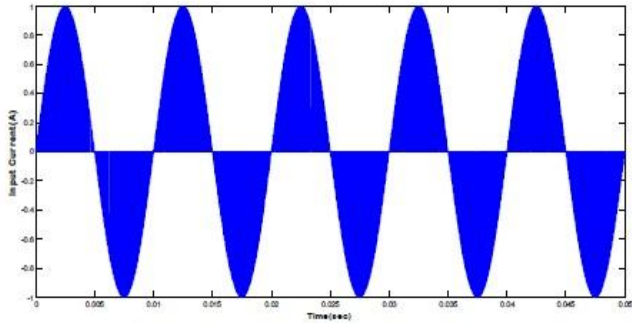


Fig.10 Input current

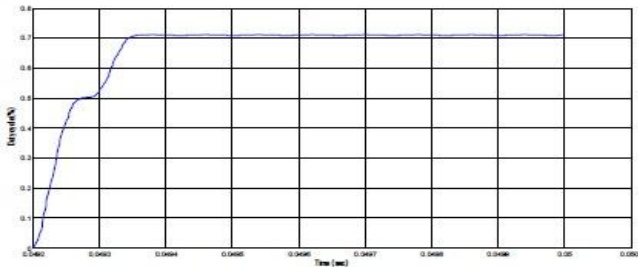


Fig.11 Duty cycle for R=200ohms

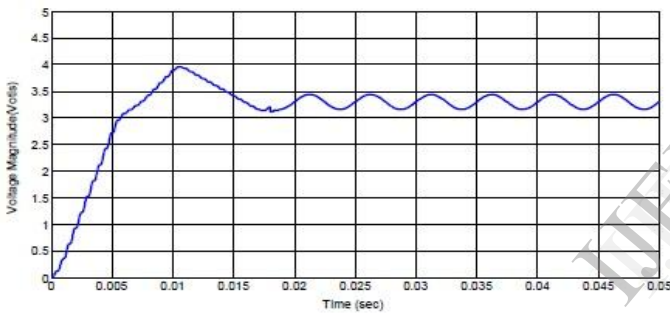


Fig.12 Output voltage for R=200ohms

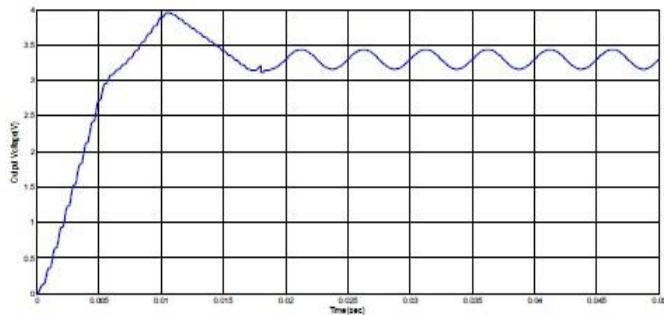


Fig.13 Output voltage for R=400ohms

Circuit Components	Name	Ratings
Inductor	$L_1, L_2$	4.7 $\mu$ H
Inductor resistance	$R_1$	30m $\Omega$
N-channel MOSFET	$S_1, S_2$	20V, 2A
MOSFET on state resistance	$R_{ds\_on}$	150 $\Omega$ @ $V_{gs}=3V$
Schottky Diode	$D_1, D_2$	23V, 1A
Schottky Diode forward voltage	$V_f$	0.23V
Load resistance	R	200 $\Omega$
Capacitor	C	68 $\mu$ F
Capacitor ESR	$R_c$	30m $\Omega$

Table1: Circuit Components

### 9. MATLAB CIRCUIT

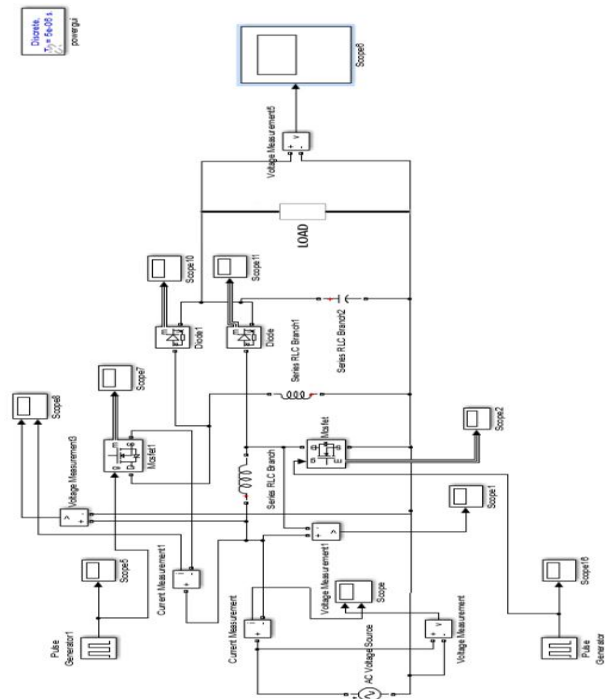


Fig.14 Matlab Circuit

The figure given below is the matlab circuit for simulation of energy harvester. All the components are extracted from simulink and blocks are prepared. The blocks are connected according to current flow. The pulse generators are used to power the gates of the mosfets. The circuit gets completed and the required voltage of 3-4 volts is obtained.

## 10. CONCLUSION

The presented direct ac-to-dc low voltage energy harvesting converter avoids the conventional bridge rectification and achieves higher efficiency. The proposed converter consists of a boost converter in parallel with a buck-boost converter. The negative gain of the buck-boost converter is utilized to boost the voltage of the negative half cycle of the microgenerator to positive dc voltage. Analysis of the converter for direct ac-to-dc power conversion is carried out and the relations between various converter circuit parameters and control parameters are obtained. The measured efficiency of the converter is 61% which is higher than the reported converters.

## REFERENCES

1. J. A. Paradiso and T. Starner, "Energy scavenging for mobile and wireless electronics," *IEEE Pervasive Comput.*, vol. 4, no. 1, pp. 18–27, Jan./Mar.2005.
2. S. Meninger, J. O. Mur-Miranda, R. Amirtharajah, A. P. Chandrakasan, and J. H. Lang, "Vibration-to-electric energy conversion," *IEEE Trans. Very Large Scale Integr. Syst.*, vol. 9, no. 1, pp. 64–76, Feb. 2001.
3. M. El-Hami, P. Glynn-Jones, N. M. White, M. Hill, S. Beeby, E. James, A. D. Brown, and J. N. Ross, "Design and fabrication of a new vibration based electromechanical power generator," *Sens. Actuators A: Phys.*, vol. 92, pp. 335–342, 2001.
4. T. M. Thul, S. Dwari, R. D. Lorenz, and L. Parsa, "Energy harvesting and efficient power generation from human activities," in *Proc. Center Power Electron. Syst. (CPES) Semin.*, Apr. 2007, pp. 452–456.
5. N. G. Stephen, "On energy harvesting from ambient vibration," *J. Sound Vibrations*, vol. 293, pp. 409–425, 2006.
6. J. R. Amirtharajah and A. P. Chandrakasan, "Self-powered signal processing using vibration-based power generation," *IEEE J. Solid-State Circuits*, vol. 33, no. 5, pp. 687–695, May 1998.
7. B. H. Stark, P. D. Mitcheson, M. Peng, T. C. Green, E. Yeatman, and A. S. Holmes, "Converter circuit design, semiconductor device selection and analysis of parasitics for micro power electrostatic generators," *IEEE Trans. Power Electron.*, vol. 21, no. 1, pp. 27–37, Jan. 2006.
8. C. B. Williams and R. B. Yates, "Analysis of a micro-electric generator for micro systems," in *Proc. Int. Conf. Solid-State Sens. Actuators*, 1995, pp. 369–372.
9. P.D.Mitcheson, T.C.Green, E.M.Yeatman, and A. S. Holmes, "Architectures for vibration-driven micro power generators," *J. Micro electro mech.Syst.*, vol. 13, no. 3, pp. 429–440, Jun. 2004.
10. S. Xu, K. D. T. Ngo, T. Nishida, G. B. Chung. Sharma, "Low frequency pulsed resonant converter for energy harvesting," *IEEE Trans. Power Electron.*, vol. 22, no. 1, pp. 63–68, Jan. 2007. J. Elmes, V. Gaydarzhiev, A. Mensah, K. Rustom, J. Shen, and I. Batarseh, "Maximum energy harvesting control for oscillating energy harvesting systems," in *Proc. IEEE Power Electron. Spec. Conf.*, Jun. 2007, pp. 2792–2798.
11. S. P. Beeby, R. N. Torah, M. J. Tudor, P. Glynn-Jones, T. O'Donnell, C. R.Saha, and S. Roy, "Micro electromagnetic generator for vibration energy harvesting," *J. Micromech. Microeng.*, vol. 17, pp. 1257–1265, 2007.
12. B. H. Stark, P. D. Mitcheson, M. Peng, T. C. Green, E. Yeatman, and A. S. Holmes, "Converter circuit design, semiconductor device selection and analysis of parasitics for

micro power electrostatic generators," *IEEE Trans. Power Electron.*, vol. 21, no. 1, pp. 27–37, Jan. 2006.

## AUTHORS PROFILE



**G.SRIDHAR BABU**, presently working as Assistant professor in St Martin's Engineering College, Hyderabad, Andhra Pradesh India. He received the B.Tech degree in Electrical & Electronics Engineering from JNTUH,

Hyderabad in 2003. And then completed his P.G in Electrical & Electronics Engineering as Power electronics specialization at JNTUH, Hyderabad in 2006. He has authored 5 papers published in national and international journals. His area of interest includes are Power Electronic Drives control, PWM Theory and fuzzy logic controllers. He is the life time member of ISTE.



Vishal Mishra has completed his graduation from St. Martin's engineering college, Hyderabad, Andhra Pradesh, India. His field of interest includes power electronics and power systems.



G.Suresh Kumar has completed his graduation from St. Martin's engineering college, Hyderabad, Andhra Pradesh, India. His field of interest includes power electronics, power systems and control systems.